COMPRESSED BEAMFORMING WITH APPLICATIONS TO ULTRASOUND IMAGING

Noam Wagner[⋆] *Yonina C. Eldar*[⋆] *Arie Feuer*[⋆] *Zvi Friedman*[⋆†]

[⋆] Technion-Israel Institute of Technology, Technion City, Haifa, Israel
[†] GE Health-care, Haifa, Israel

ABSTRACT

Recent developments in medical treatment put challenging demands on ultrasound imaging systems. These demands typically imply increasing the number of transducer elements involved in each imaging cycle. Confined to traditional sampling methods, the inevitable result is a significant growth in the amount of raw data that needs to be transmitted from the system front end, and then processed by the processing unit, effecting machinery size and power consumption. In this paper, we derive a scheme which reduces the amount of transmitted data, by applying Compressed Sensing (CS) techniques to analog ultrasound signals detected in the transducer elements. We follow the spirit of Xampling, which combines classic methods from sampling theory with recent developments in CS, aimed at sampling analog signals far below the Nyquist rate. Our scheme enhances SNR, by integrating low-rate samples extracted from multiple transducer elements. We refer to this process as "beamforming in the compressed domain", or "compressed beamforming".

Index Terms— Array Processing, Beamforming, Compressed Sensing (CS), Dynamic Focus, Finite Rate of Innovation (FRI), Matrix Pencil, Ultrasound, Xampling

1. INTRODUCTION

In ultrasound-based diagnostic imaging, ultrasonic pulses are transmitted into the scanned tissue. Reflections of the transmitted energy, caused by density and propagation-velocity perturbations in the tissue [1], are then measured by an array of transducer elements. Applying the acoustic reciprocity theorem, data from multiple elements is digitally integrated in the processing unit, in a process known as beamforming [2], which results in significant SNR enhancement. Digital beamforming requires sampling the signals detected in all active elements, and then transmitting the samples to the processing unit. Confined to the classic Nyquist-Shannon theorem [3], traditional methods require that this data be sampled at twice the baseband bandwidth of the detected signals. Avoiding artifacts, caused by the digital implementation, requires that the data be sampled at even higher rates, typically 3-5 times the center frequency of the transmitted pulse [2]. Sampling at such rates is not necessarily a bottleneck in modern systems. On the other hand, as imaging techniques evolve, the number of elements involved in each imaging cycle grows significantly. Consequently, large amounts of data must be transmitted to the processing unit, posing an engineering challenge. This motivates compression of the sampled data, before its transmission to the processing unit.

In their recent work, Tur et. al. [4] propose that the ultrasound signal detected by each receiver be regarded as Finite Rate of Innovation (FRI) [5, 6]. More explicitly, they model it as L replicas of a known-shape pulse, caused by scattering of the transmitted pulse from point reflectors, located along the narrow transmission beam. Applying the FRI framework, [4, 7] propose two robust schemes, which enable reconstruction of the signal, characterized by $2L$ degrees of freedom, from samples taken at a rate far below Nyquist. Combining classic sampling methods with recent CS developments, these schemes follow the spirit of Xampling [8]. Nevertheless, applying such schemes to signals originating in biological tissues, often results in erroneous parameter estimation, due to the noisy nature of numerous reflections from microscopic scatterers.

The goal of our work is to design a Xampling scheme, which achieves substantial SNR enhancement of the data, by integrating low-rate samples from multiple elements. We refer to this process as "Beamforming in the Compressed Domain", since it exploits ideas from traditional beamforming. We propose two compressed beamforming schemes. Applying these schemes to real ultrasound data, we successfully image macroscopic perturbations, embedded in the scanned plane, while achieving a ten-fold reduction in sampling rate, compared to standard imaging techniques. The first scheme extracts the necessary low rate samples using multiple modulation and integration channels, applied to the analog signal detected in each receiver. The second scheme approximates these samples, based on frequency samples of the detected signals. It thus achieves similar performance to the first scheme, in terms of sampling rate and image quality, while utilizing a much simpler sampling mechanism.

This paper is organized as follows: in Section 2, we review the principles of beamforming in ultrasound imaging. In Section 3 we discuss the FRI signal model and examine beamforming in this context. We then introduce a first multiple-element Xampling scheme which integrates beamforming from low rate samples. This scheme involves complicated hardware, and we therefore introduce, in Section 4, a second Xampling scheme, which achieves similar performance to the first, while utilizing a simple compressed beamforming mechanism. In Section 5 we introduce experimental results.

2. BEAMFORMING WITH MULTIPLE RECEIVERS

We begin by describing the beamforming process, carried out in B-mode ultrasound imaging. The analysis, based mainly on [1], focuses on a linear transducer array, and may be extended to other antennae array applications.

Consider a set of M receivers, located along the $\mathbf{x}$ axis, as illustrated in Figure 1. Denote by δ_m the distance between the mth receiver and the origin, $x = 0$. Assume a pulse of energy, transmitted along the $\mathbf{z}$ axis. The pulse propagates at velocity c, such that at time t the energy is concentrated at $(x, z) = (0, ct)$. A point reflector located at this position scatters a portion of the energy, such that a pulse will be detected by every sensor, at a time instance which depends on its location. Denote by $\tau_m(t)$, the time of detection by the mth sensor, and by γ_m, the ratio δ_m/c. It may be shown that:

$$\tau_m(t) = t + \sqrt{\gamma_m^2 + t^2}. \tag{1}$$

A common SNR enhancement technique involves averaging signals detected by multiple receivers. Applying this technique here, we must first compensate for the variation in detection-time of reflections corresponding to the same scattering element. We thus set the receiver satisfying $\delta_m = 0$ as reference, denoting its index by m_0. Using (1), the detection time in this receiver takes the simple form $\tau_{m_0}(t) = 2t$, with the corresponding detection time in the mth receiver being $\tau_m(t)$. In order to align these instances, we now construct the signal $\hat{\varphi}_m(t)$ such that $\hat{\varphi}_m(2t) = \varphi_m(\tau_m(t))$. Substituting $2t \to t$, we obtain:

$$\hat{\varphi}_m(t) = \varphi_m\left(t/2 + \sqrt{\gamma_m{}^2 + (t/2)^2}\right). \quad (2)$$

Having aligned corresponding reflections through this distortion, we may average the distorted signals, resulting in the beamformed signal, $\Phi(t)$:

$$\Phi(t) = \frac{1}{M}\sum_{m=1}^{M}\hat{\varphi}_m(t). \quad (3)$$

The signal $\Phi(t)$, exhibiting enhanced SNR compared to the individual signals from which it is composed, is translated to a single image line, after envelope detection. The process formulated in (2)-(3), practically implies that, at each time instance, the array is focused to the position, along the $\mathbf{z}$ axis, from which a pulse, arriving at that instance, would have originated. Notice, that our derivation assumed continuous time. In practice, modern systems implement beamforming digitally, by applying discrete delays to samples taken from the detected signals $\{\varphi_m(t)\}_{m=1}^{M}$. Confined to traditional sampling methods, these samples must be taken at a rate which is at least twice the baseband bandwidth of the detected signals. Reducing this sampling rate is the primary goal of our work.

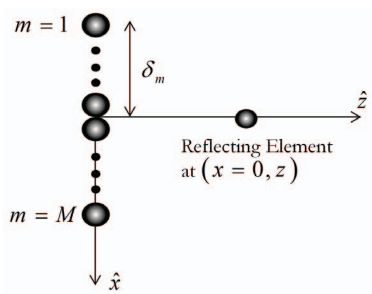

Fig. 1. Setup - M transducer elements positioned along the $\mathbf{x}$ axis. The array transmits a pulse, which encounters point reflectors as it propagates along the $\mathbf{z}$ axis.

3. BEAMFORMING SUBJECT TO THE FRI SIGNAL MODEL

Tur et. al. propose [4] that the ultrasound signal detected in an individual receiver may be considered FRI. This is based on the assumption that, as the transmitted pulse propagates, it encounters a finite set of L isolated point reflectors, aligned along the $\mathbf{z}$ axis. In the more general sense, these reflectors may be regarded as point-like, considering their intersection with the narrow transmission beam. Assuming, additionally, that we know the shape of the reflected pulse (referred to by the term "two-way" pulse), denoted by $h(t)$, the signal detected in each receiver may be approximated as:

$$\varphi_m(t) = \sum_{l=1}^{L} a_{l,m} h(t - t_{l,m}), \quad (4)$$

where $t_{l,m}$ denotes the time in which a reflection, originating from the lth reflector, arrives at the mth receiver, and $a_{l,m}$ denotes the attenuation of this reflection. The model (4) implies, that the signal detected in each receiver satisfies the FRI property [5], and may therefore be reconstructed from a minimal number of $2L$ samples.

Nevertheless, applying a Xampling scheme such as the one proposed in [4] to signals originating from biological tissues, will often result in erroneous parameter estimation, mainly due to multiple reflections from microscopic scatterers, manifested as noise. In extreme scenarios, where the noise masks the FRI component, the extracted parameters will be meaningless, and any attempt to cope with errors in the parametric space will turn out useless. However, recall that we may significantly attenuate the noise, by applying the beamforming process described in Section 2 to the individual signals. Subject to the signal model proposed here-above, if the resulting beamformed signal, $\Phi(t)$, additionally maintains the FRI property, then there is obvious advantage in applying the Xampling scheme to this signal, rather than to the individual signals from which it is generated.

Assuming that all reflections originate from points along the $\mathbf{z}$ axis, we can show that, to good approximation, $\Phi(t)$ may be approximated as:

$$\Phi(t) \approx \sum_{l=1}^{L}\left(\frac{1}{M}\sum_{m=1}^{M} a_{l,m}\right) h(t - t_l) = \sum_{l=1}^{L} b_l h(t - t_l), \quad (5)$$

with t_l being the delay measured by the reference receiver, m_0, for a reflection originating from the lth reflector, that is: $t_l := t_{l,m_0}$. We emphasize the invariance to m in the last formulation, rising from the fact that the distortion applied by (2) aligns reflections originating from the same point along the path of the transmitted pulse. Since it additionally distorts the shape of the reflected pulse, (5) holds only approximately.

Having approximated $\Phi(t)$ as FRI, comprising L replicas of a known-shape pulse, we can now apply FRI sampling to (5). However, recall that $\Phi(t)$ does not exist in the analog domain. Thus, our problem is how to obtain samples of (5), where in practice all we have access to are the individual signals $\{\varphi_m(t)\}_{m=1}^{M}$.

Beginning our derivation, let us conceptually feed $\Phi(t)$ into the FRI Xampling scheme proposed in [7]. This scheme may be divided into two separate blocks: the first, operating in the analog domain, extracts a subset of the signal's Fourier coefficients. The subset comprises K consecutive coefficients, where $K \geq 2L$. Denote the sequence of these coefficients' indexes by $\kappa = \{k_1, k_2, ..., k_K\}$; the second block, operating in the digital domain, estimates the unknown signal parameters from the Fourier coefficients extracted by the first block, by applying spectral estimation techniques such as annihilating filter [9]. In the following sections, we confine our discussion to the first block, where our goal is to extract the sequence κ of $\Phi(t)$'s Fourier coefficients.

Consistent with [7], our first Xampling block consists of K branches, each comprising a modulating kernel and an integrator. We set the integration interval to be $[0, T)$, choosing T according to the transmitted pulse's penetration depth, such that the interval contains the support of $\Phi(t)$. We farther require, that the integration interval contains the support of $\varphi_m(t)$, for every $1 \leq m \leq M$.

It may be shown, that the support of $\varphi_m(t)$ is bounded from below by $\gamma_m \geq 0$. Denoting the upper bound of this support by T_m (once again dictated by the penetration depth), we select T such that it additionally satisfies $T \geq \max_{1\leq m\leq M} T_m$. Without loss of generality, we choose the modulating kernel in the jth branch to be $e^{-j\frac{2\pi}{T}k_j t}$, k_j being the jth element in κ. With this choice, the output of this branch is simply $\Phi(t)$'s k_jth Fourier coefficient:

$$c_j = \int_0^T e^{-i\frac{2\pi}{T}k_j t}\Phi(t)dt. \tag{6}$$

Substituting $\Phi(t)$, expressed in (2)-(3), into (6), we now get:

$$\begin{aligned} c_j &= \frac{1}{M}\int_0^T e^{-i\frac{2\pi}{T}k_j t}\sum_{m=1}^{M}\hat{\varphi}_m(t)dt \\ &= \frac{1}{M}\sum_{m=1}^{M}\int_0^T e^{-i\frac{2\pi}{T}k_j t}\varphi_m\left(t/2+\sqrt{\gamma_m{}^2+(t/2)^2}\right)dt \\ &= \frac{1}{M}\sum_{m=1}^{M}c_{j,m}, \end{aligned} \tag{7}$$

where

$$c_{j,m} = \int_0^T g_{j,m}(t)\varphi_m(t)\,dt, \tag{8}$$

and

$$\begin{aligned} g_{j,m}(t) &= q_{j,m}(t)e^{-i\frac{2\pi}{T}k_j t}, \\ q_{j,m}(t) &= I_{[\gamma_m,T_m)}(t)\left(1+\gamma_m{}^2/t^2\right)e^{i\frac{2\pi}{T}k_j\frac{\gamma_m{}^2}{t}}. \end{aligned} \tag{9}$$

Here, $I_{[a,b)}(t)$ denotes an indicator function, namely:

$$I_{[a,b)}(t) = \begin{cases} 1 & a \leq t < b \\ 0 & \text{otherwise} \end{cases}. \tag{10}$$

The process defined in (7)-(10) describes a desired combination of the beamforming with the first stage of the Xampling, and is depicted in Figure 2. Each received signal, $\varphi_m(t)$, is multiplied by a bank of kernels, $\{g_{j,m}(t)\}_{j=1}^K$, defined by (9), and integrated over the interval $[0,T)$, resulting in a vector $\mathbf{c_m} = \begin{bmatrix} c_{1,m} & c_{2,m} & \dots & c_{K,m}\end{bmatrix}^T$. The vectors $\{\mathbf{c_m}\}_{m=1}^M$ are then averaged in $\mathbf{c} = \begin{bmatrix} c_1 & c_2 & \dots & c_K\end{bmatrix}^T$, which has the desired improved SNR property and provides the basis for extracting the $2L$ parameters of $\Phi(t)$, the second stage of the Xampling. Assuming that the estimated number of pulses, L, satisfies $L \ll f_s T$, where f_s is the Nyquist frequency, dictated by the bandwidth of the detected signals, then we may obtain beamforming using samples taken at a rate which is far below the Nyquist rate.

4. SIMPLIFYING THE XAMPLING MECHANISM

Implementing the scheme derived in Section 3 requires complicated hardware, due to the complexity of the kernels. We now modify this scheme, such that it utilizes a much simpler sampling mechanism.

With its support contained in $[0,T)$, the FRI component, $\varphi_m(t)$, may be expressed it in terms of its possibly infinite set of Fourier coefficients, $\{\phi_m[n]\}_{n=-\infty}^{\infty}$, calculated with respect to this interval. Let us approximate $\varphi_m(t)$ using just a finite subset of consecutive

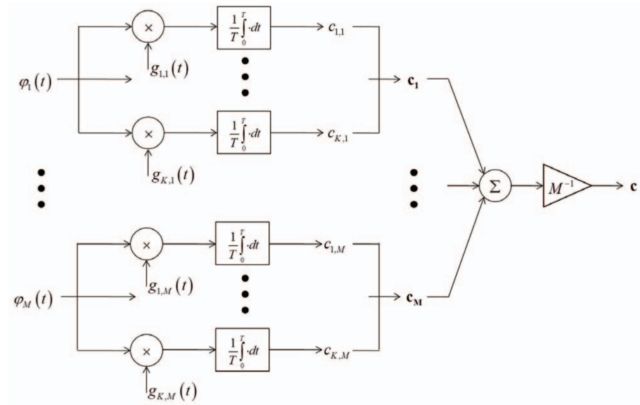

Fig. 2. Xampling scheme utilizing distorted exponential kernels.

coefficients. Substituting this approximation into (8), with $g_{j,m}(t)$ defined in (9), yields:

$$\hat{c}_{j,m} = \sum_{n=N_1}^{N_2}\phi_m[k_j-n]Q_{j,m}[n], \tag{11}$$

where $Q_{j,m}[n]$ are the Fourier series for $q_{j,m}(t)$, which is also defined on the interval $[0,T)$. It can be shown that, for any given $\epsilon > 0$, for any pair (j,m), there exist $N_1(\epsilon,k_j,m)$ and $N_2(\epsilon,k_j,m)$ such that $|\hat{c}_{j,m} - c_{j,m}| < \epsilon$, and so with the finite sum (11), we may approximate $c_{j,m}$ to any accuracy. Furthermore, setting an upper bound on the energy of $\varphi_m(t)$, N_1 and N_2 may be chosen subject to the decay properties of the sequence $\{Q_{j,m}[n]\}_{n=-\infty}^{\infty}$, and can be done off-line.

We may now design a modified sampling scheme, for estimating the chosen set of $\Phi(t)$'s Fourier coefficients, $\{c_j\}_{j=1}^K$. Setting the desired accuracy of approximation, ϵ, we first calculate the pair $N_1(\epsilon,k_j,m)$ and $N_2(\epsilon,k_j,m)$ for every $1 \leq j \leq K$ and $1 \leq m \leq M$. Given such pair, denote by $\kappa_{k_j,m}$ the sequence of indexes corresponding to $\varphi_m(t)$'s Fourier coefficients, participating in (11). Namely, $\kappa_{k_j,m} = \{k_j - n\}_{n=N_1(\epsilon,k_j,m)}^{N_2(\epsilon,k_j,m)}$. Additionally, denote by κ_m, the union $\cup_{j=1}^K \kappa_{k_j,m}$, with K_m being the number of elements in this union. The modified sampler will extract the sequence $\{\phi_m[k]\}_{k\in\kappa_m}$ from the signal detected in the mth receiver. A linear transformation will now be applied to this sequence, resulting in the ϵ-approximation of the coefficients $\{c_{j,m}\}_{j=1}^K$. Writing this transformation in matrix form, we have:

$$\mathbf{\hat{c}_m} = \mathbf{A_m\Phi_m}, \tag{12}$$

where $\mathbf{\hat{c}_m}$ is the length K vector containing $\hat{c}_{j,m}$ as its jth element, $\mathbf{\Phi_m}$ is the length K_m vector containing the kth coefficient of the sequence $\{\phi_m[k]\}_{k\in\kappa_m}$ as its kth element, and $\mathbf{A_m}$ is a $K \times K_m$ matrix, constructed as follows:

$$\mathbf{A_m}[j,k] = \begin{cases} Q_{j,m}\left(\frac{2\pi}{T}(k_j - \kappa_m\{k\})\right) & \kappa_m\{k\} \in \kappa_{k_j,m} \\ 0 & \text{otherwise} \end{cases}. \tag{13}$$

Here $\kappa_m\{k\}$ denotes the kth element in the sequence κ_m. The resulting Xampling scheme is illustrated in Figure 3. In our first scheme, depicted in Figure 2, the samples taken in each receiver required that the corresponding signal be fed into K branches, in which it was modulated using a complicated set of kernels. In the current scheme, however, a much simpler sampling mechanism may be used, namely: a linear transformation, $\mathbf{V_m}$, is applied to pointwise samples of the signal, taken at sub-Nyquist rate, after filtering it with an appropriate kernel, $s_m^*(-t)$, such as the Sum of Sincs [4].

Concluding this section, let us consider a setup, in which the sampled signal is band-limited, and may be sampled at Nyquist rate in each receiver. This is, in fact, often the case in ultrasound systems. In such case, implementing the linear transformation (12) at the level of each receiver, the approximation error vanishes, while reducing the transmission rate to that achieved by our first scheme.

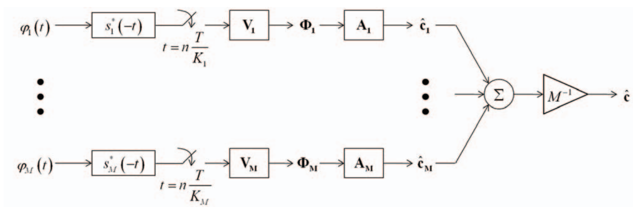

Fig. 3. Xampling scheme utilizing Fourier samples of detected signals.

5. SIMULATION ON ULTRASOUND DATA

We examine the result of applying our proposed schemes to raw RF ultrasound data. The data was acquired using a programmable imaging system (Model V-1-128, Verasonics, Inc., Redmond, WA), equipped with a 128-element 1-D linear transducer array (Model L7-4, Philips Healthcare, Bothell, WA). The imaging target was a commercial multi-purpose gray-scale phantom (Model 403GS LE, Gammex, Inc., Middleton, WI) including 0.1-mm nylon wires embedded in tissue mimicking material. Each image line is constructed from $M = 16$ active elements, distanced $\delta = 0.3$mm apart. Imaging to a depth of $z = 7.88$cm, we obtain $T = 102\mu$sec. The results are illustrated in Figure 4.

In the first experiment, we generate an image using standard techniques, applying beamforming to data sampled at the Nyquist rate. Sampling at 20MHz, a single image line requires that 2048 samples be taken in each element. We use the resulting image (a) as reference, and aim at reproducing it using our Xampling schemes. We begin by applying our first Xampling scheme. Assuming $L = 30$ reflectors, and using a factor 3 oversampling, κ comprises $K = 181$ indexes, so that we obtain over ten-fold reduction in sample rate. The resulting image (b) well depicts strong perturbations observed in (a). Notice that point reflectors, located at the proximity of the array ($z \approx 1$cm) remain well in focus, due to the integrated beamforming. We next apply our second Xampling scheme. For every $k_j \in \kappa$ and for every $1 \leq m \leq M$, we choose N_1 and N_2 of (11) such that $\sum_{n=N_1}^{N_2} \left|Q_{j,m}\left(\frac{2\pi}{T}n\right)\right|^2 \approx 0.9 \sum_{n=-\infty}^{\infty} \left|Q_{j,m}\left(\frac{2\pi}{T}n\right)\right|^2$. In our setup, this results in an average number of 190 samples per receiving element, required for constructing a single image line. We are still left with a ten-fold reduction in sample rate, where the resulting image (c) appears very similar to (b).

ACKNOWLEDGMENTS

The authors would like to thank Dr. Omer Oralkan and Prof. Pierre Khuri-Yakub of the E. L. Ginzton Laboratory at Stanford University, for providing the RF ultrasound data and for many helpful discussions.

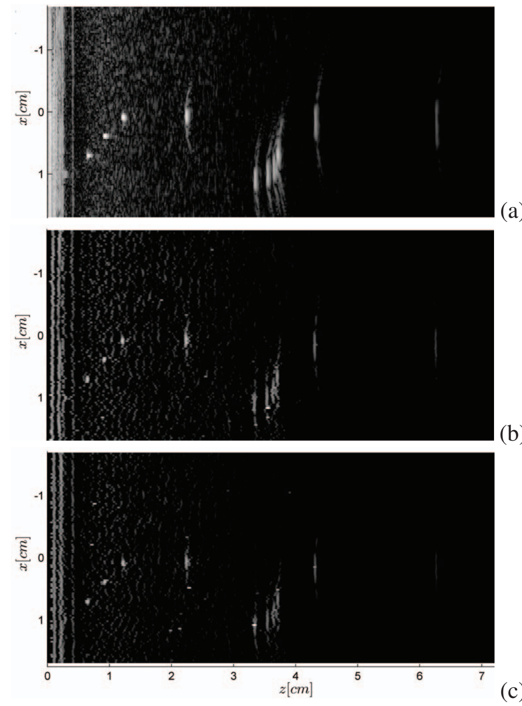

Fig. 4. Comparison of two Xampled images and an image obtained using traditional methods.

6. REFERENCES

[1] J. Arendt Jensen, "Linear description of ultrasound imaging systems," Notes for the International Summer School on Advanced Ultrasound Imaging, Technical University of Denmark, 1999.

[2] T. L. Szabo, "Diagnostics ultrasound imaging: Inside out," in *Academic Press Series in Biomedical Engineering*, Joseph Bronzino, Ed., pp. Ch. 7, 10. Elsevier Academic Press, 2004.

[3] C. E. Shannon, "Communication in the presence of noise," *Proc. IRE*, vol. 37, pp. 10 – 21, 1949.

[4] R. Tur, Y. C. Eldar, and Z. Friedman, "Innovation rate sampling of pulse streams with application to ultrasound imaging," *IEEE Trans. on Signal Processing*, vol. 59, No. 4, pp. 1827 – 1842, 2011.

[5] M. Vetterli, P. Marziliano, and T. Blu, "Sampling signals with finite rate of innovation," *IEEE Transactions on Signal Processing*, vol. 50, No. 6, pp. 1417 – 1428, 2002.

[6] T. Blu, P. L. Dragotti, M. Vetterli, P. Marziliano, and L. Coulot, "Sparse sampling of signal innovations," *IEEE Signal Process. Mag.*, vol. 25, No. 2, pp. 31 – 40, 2008.

[7] K. Gedalyahu, R. Tur, and Y. C. Eldar, "Multichannel sampling of pulse streams at the rate of innovation," *IEEE Trans. on Signal Processing*, vol. 59, No. 4, pp. 1491 – 1504, 2011.

[8] M. Mishali, Yonina C. Eldar, O. Dounaevsky, and E. Shoshan, "Xampling: Analog to digital at sub-nyquist rates," *IET Journal of Circuits, Devices and Systems*, vol. 5, Issue 1, pp. 8 – 20, 2011.

[9] P. Stoica and R. Moses, *Introduction to Spectral Analysis*, Prentice-Hall, Englewood Cliffs, NJ, 2000.